01 Jan 2022

Single-Snapshot Localization for Near-Field Ris Model using Atomic Norm Minimization

Omar Rinchi

Ahmed Elzanaty

Ahmad Alsharoa
Missouri University of Science and Technology, aalsharoa@mst.edu

Recommended Citation

O. Rinchi et al., "Single-Snapshot Localization for Near-Field Ris Model using Atomic Norm Minimization," *2022 IEEE Global Communications Conference, GLOBECOM 2022 - Proceedings*, pp. 2432 - 2437, Institute of Electrical and Electronics Engineers, Jan 2022.
The definitive version is available at https://doi.org/10.1109/GLOBECOM48099.2022.10000689

Single-Snapshot Localization for Near-Field RIS Model Using Atomic Norm Minimization

Omar Rinchi
Missouri University of Science and Technology
Rolla, MO, USA
Email: omar.rinchi@mst.edu

Ahmed Elzanaty
University of Surrey
Guildford, United Kingdom
Email: a.elzanaty@surrey.ac.uk

Ahmad Alsharoa
Missouri University of Science and Technology
Rolla, MO, USA
Email: aalsharoa@mst.edu

GLOBECOM 2022 - 2022 IEEE Global Communications Conference | 978-1-6654-3540-6/22/$31.00 ©2022 IEEE | DOI: 10.1109/GLOBECOM48099.2022.10000689

***Abstract*—Reconfigurable intelligent surfaces (RISs) are expected to play a significant role in the next generation of wireless cellular technology. This paper proposes an uplink localization scheme using a single-snapshot solution for user equipment (UE) that is located in the near-field of the RIS. We propose utilizing the atomic norm minimization method to achieve super-resolution localization accuracy. We formulate an optimization problem to estimate the UE location parameters (i.e., angles and distances) by minimizing the atomic norm. Then, we propose to exploit strong duality to solve the atomic norm problem using the dual problem and semidefinite programming (SDP). The RIS is controlled and designed using estimated parameters to enhance the beamforming capabilities. Finally, we compare the localization performance of the proposed atomic norm minimization with compressed sensing (CS) in terms of the localization error. The numerical results show a superior performance of the proposed atomic norm method over the CS where a sub-cm level of accuracy can be achieved under some of the system configuration conditions using the proposed atomic norm method.**

***Index Terms*—Reconfigurable Intelligent Surface (RIS); near-field; wireless localization; atomic norm minimization; semidefinite programming (SDP);**

I. Introduction

Wireless localization is attracting booming interest in the last couple of years due to the recent developments in the capabilities of wireless networks. For instance, the next 5G+ and 6G networks aim to consider high-frequency bands such as the millimeter-wave (mm-wave) and wider bandwidths. This will allow conducting a fine and super-resolution localization [1], [2]. However, with high frequencies, new challenges arise such as the blockage of the line-of-sight (LOS) communications [3]–[5]. As a solution to these challenges, reconfigurable intelligent surfaces (RISs) have been introduced as a promising energy-efficient solution to solve the high shadowed LOS communications under high-frequency bands. The RIS is a low-cost and low-power meta-material surface that can steer the received signal toward a target direction [6], [7]. With careful RIS optimization, the high shadowed LOS links can be enhanced by creating strong non-direct LOS links between the transmitters and receivers through the RIS.

Localization and communication under short distances where the wavefront of the received signal has a considerable curvature violate the planner wavefront assumption that is used in the far-field. Such a spherical wavefront can promote the channel model to a more complicated format known as the near-field model. The Fraunhofer distance that is proportionally function of both the carrier frequency and the aperture size can be used as a threshold to define the near-field region where any wireless communications below this threshold are considered a near-field. Adopting high frequencies in the next wireless systems will not only push up the near-field threshold as the Fraunhofer distance implies [8]. However, it will also lead to high path losses that will promote short-range communications and hence, communication under the Fraunhofer threshold [9]. Furthermore, large surfaces such as the RIS and future massive multiple-input multiple-output (MIMO) systems can support the near-field claims as they increase the Fraunhofer threshold [10].

Several works in the literature have investigated RIS-aided near-field localization. For instance, in [10] the error bounds for a RIS-aided near-field 3D localization and orientation estimation were proposed using the Cramér-Rao lower bound (CRLB). Similar work has been done in [11], where the authors derived the error bounds for the near-field RIS-aided model and recommended the best system configurations that can improve the localization continuity. However, non of the above-mentioned works consider proposing a practical localization scheme for near-field models. In that regard, the authors in [12] proposed a near-field localization for RIS-aided models. The localization algorithm is based on a two-step approach in which the time of arrival (ToA) is first estimated and then followed by the user equipment (UE) localization. Additionally, in [13] the authors considered a compressed sensing (CS)-based localization for a near-field and multi-path model, however, the adopted CS algorithm suffers from high-localization errors due to the quantization errors. Both [12] and [13] considered their localization algorithms for a multiple-snapshots solution only which can be impractical, especially for dynamically movable systems and low coherence time channels. To the best of our knowledge, localization with using a single-snapshot solution for a UE that is located in the near-field of the RIS is still lacking in the literature.

In this paper, we propose to exploit the sparsity in the mm-wave to estimate the location of a UE located in the near-field of a RIS in terms of its angle of departure (AoD) and distance with respect to the RIS using only a single-snapshot. We utilize atomic norm minimization-based technique to achieve super-resolution localization accuracy and solve the quantization error problems compares to the conventional CS sparse recovery techniques. The contributions of this paper can be summarized as follows:

- We propose a super-resolution localization scheme using a single-snapshot for a UE that is located in the near-field of RIS.
- We formulate an optimization problem to estimate the UE location parameters (i.e., angles and distances) based on the atomic norm minimization.
- Due to the complexity of the optimization problem, we drive the dual norm and convert the problem to a convex semidefinite programming (SDP) problem.
- We propose low complexity algorithms to extract the location information from the Lagrangian variable compare it with the exhaustive search (ES).

Notation: We represent all the matrices as capital and bold letters $\mathbf{X}$, vectors are represented as bold and lowercase letter $\mathbf{x}$, and scalars are represented as non-bold letters x or X. The transpose, conjugate, pseudo-inverse, and Hermitian transpose operators are given as $(.)^T$, $(.)^*$, $(.)^\dagger$, and $(.)^H$, respectively. We use diag(.) to convert a vector into a diagonal matrix, tr(.) to compute the trace of a matrix, $\mathbf{I}_{N^{\mathrm{U}}}$ to represent and identity matrix of size N^{U}, $||.||_\ell$ to represent the operator that computes the ℓ^{th} norm, and Re(.) to compute the real value of a complex number. For matrix $\mathbf{X}$, we use $\mathbf{x}_l$ and $x_{b,l}$ to represent the l^{th} column and b^{th} element, respectively.

II. System Model

We consider a localization system that consists of a UE, base station (BS), and RIS which are located at $\mathbf{p}^{\mathrm{U}} = [x^{\mathrm{U}}, y^{\mathrm{U}}]^T$, $\mathbf{p}^{\mathrm{B}} = [x^{\mathrm{B}}, y^{\mathrm{B}}]^T$, and $\mathbf{p}^{\mathrm{R}} = [x^{\mathrm{R}}, y^{\mathrm{R}}]^T$, respectively. We consider MIMO system where the number of antennas in the UE, BS, and the RIS are given as $N^{\mathrm{U}}, N^{\mathrm{B}}$, and N^{R}, respectively. We assume that all the stations are equipped with uniform linear arrays (ULAs). Our model focus on uplink poisoning where the BS retrieves the location of the UE from its uplink signal arrived through the RIS as shown in Fig. 1. Further, we assume that the LOS between the BS and the UE is blocked.

The received signal model at the BS is expressed as

$$\mathbf{Y} = \mathbf{H}\,\mathbf{X} + \mathbf{Z}, \tag{1}$$

where $\mathbf{Y}$ is the received signal, $\mathbf{X} \in \mathbb{C}^{N^{\mathrm{U}} \times M^{\mathrm{o}}}$ represents the positioning reference signal (PRS) with M^{o} column pilots that are orthogonal having power P, i.e, $\mathbf{X}\mathbf{X}^{\mathrm{H}} = \frac{P}{N^{\mathrm{U}}}\mathbf{I}_{N^{\mathrm{U}}}$, and $\mathbf{Z} \in \mathbb{C}^{N^{\mathrm{B}} \times M^{\mathrm{o}}}$ represents the additive white Gaussian noise (AWGN) where $z_{i,j} \sim \mathcal{CN}(0, \sigma_z^2)$. The overall channel matrix between the UE and the BS $\mathbf{H}$ can be modeled as [14]

$$\mathbf{H} = \mathbf{H}^{\mathrm{BR}}\mathrm{diag}(\boldsymbol{\Theta})\mathbf{H}^{\mathrm{UR}}, \tag{2}$$

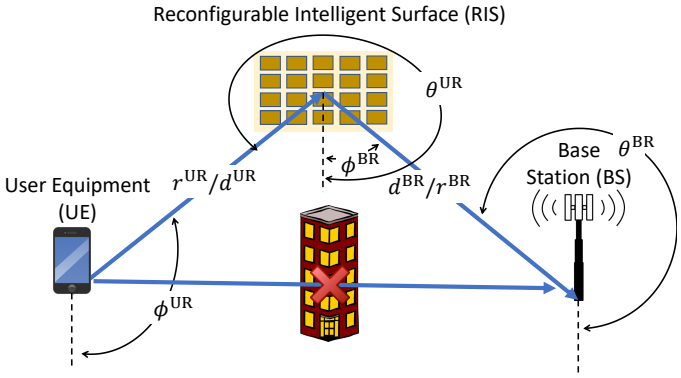

Fig. 1: The proposed system scenario and architecture.

where $\mathrm{diag}(\boldsymbol{\Theta}) \in \mathbb{C}^{N^{\mathrm{R}} \times N^{\mathrm{R}}}$ is a matrix that represents the phase control of the RIS where $\boldsymbol{\Theta} \triangleq \left[\zeta_1 e^{j\theta_1}, \zeta_2 e^{j\theta_2}, \cdots, \zeta_{N^{\mathrm{R}}} e^{j\theta_{N^{\mathrm{R}}}}\right]^T$ where $\zeta_r = 1$ as we consider ideal RIS, and $\mathbf{H}^{\mathrm{BR}} \in \mathbb{C}^{N^{\mathrm{B}} \times N^{\mathrm{R}}}$ represents the channel between the RIS and the BS while $\mathbf{H}^{\mathrm{RU}} \in \mathbb{C}^{N^{\mathrm{R}} \times N^{\mathrm{U}}}$ is the channel between the UE and the RIS. More specifically

$$\mathbf{H}^{\mathrm{BR}} = \mathbf{a}(\theta^{\mathrm{BR}}, d^{\mathrm{BR}})\,\rho^{\mathrm{BR}}\,\mathbf{a}^H(\phi^{\mathrm{BR}}, r^{\mathrm{BR}}), \tag{3}$$

where $\mathbf{a}(\theta^{\mathrm{BR}}, d^{\mathrm{BR}})$ and $\mathbf{a}^H(\phi^{\mathrm{BR}}, r^{\mathrm{BR}})$ represents the steering vectors at the BS and the RIS respectively, the angles ϕ^{BR} and θ^{BR} are the AoD and the angle of arrival (AoA), on the other hand both r^{BR} and d^{BR} represents the distance between the RIS and the BS[1]. We can use the Fresnel approximation to model the spherical wavefront in the near-field model as [15]

$$a_b(\theta^{\mathrm{BR}}, d^{\mathrm{BR}}) = \exp\left(j\left[b\,\omega^{\mathrm{BR}} + b^2\,\gamma^{\mathrm{BR}}\right]\right), \tag{4}$$

where $\omega^{\mathrm{BR}} \triangleq f(\theta^{\mathrm{BR}})$ and $\gamma^{\mathrm{BR}} \triangleq g(\theta^{\mathrm{BR}}, d^{\mathrm{BR}})$ with

$$f(\phi) = -\frac{2\pi\delta}{\lambda}\sin(\phi), \quad g(\phi, r) = \frac{\pi\delta^2}{\lambda\, r}\cos^2(\phi), \tag{5}$$

where λ is the wavelength as $\lambda = c/f_c$, f_c is the carrier frequency and c is the speed of light, δ is a fixed distance between each of adjacent elements in the ULA, $\rho^{\mathrm{RB}} \in \mathbb{C}$, represents the propagation gain between the RIS and BS which can be expressed as

$$\rho^{\mathrm{BR}} = \left(\frac{c}{4\pi(r^{\mathrm{BR}} + d^{\mathrm{BR}})f_c}\right)^{\frac{\mu}{2}}\mathcal{F}, \tag{6}$$

where $\mathcal{F}$ is a random variable representing the fading and modelled as a standard complex Gaussian, μ is the path loss exponent. The channel model between the UE and the RIS $\mathbf{H}^{\mathrm{UR}}$ is modeled in a similar way.

III. RIS-aided super-resolution localization

The goal is to estimate the UE location using the aid of the RIS. We utilize the atomic norm minimization to estimate the localization parameters $(\phi^{\mathrm{UR}}, r^{\mathrm{UR}}, \theta^{\mathrm{BR}}, d^{\mathrm{BR}})$ using the received signal; we then exploit the estimated parameters to design the RIS control matrix. We now re-estimate the parameters after adjusting RIS control to enhance the localization accuracy.

[1]This is a special case of the multi-path case where $\boldsymbol{r}^{\mathrm{BR}}$ and $\boldsymbol{d}^{\mathrm{BR}}$ are the distances between (BS and scatterees) and (RIS and scatterees) respectively.

A. Estimation of the Localization Parameters

Let us define the atomic set in $\mathbf{H}^{\text{UR}}$ as

$$\mathcal{A} \triangleq \{\mathbf{a}^{\text{UR}}\left(\phi^{\text{UR}}, r^{\text{UR}}\right) | \phi^{\text{BR}} \in \quad [-\frac{\pi}{2}, \frac{\pi}{2}), r^{\text{UR}} \in [0, R)\}. \quad (7)$$

The set $\mathcal{A}$ in (7) is refers to the atomic set as it is a set on the continuous domain that has all the possible atoms. Knowing the exact atoms leads to knowing the angles that this atom is made of and, hence, estimating the location. Define $||\hat{\mathbf{h}}||_{\mathcal{A},0}$ to be the atomic l_0 norm such that

$$||\hat{\mathbf{h}}||_{\mathcal{A},0} \triangleq \inf_{L}\{L : \hat{\mathbf{h}} = \sum_{l=1}^{L} \mathbf{a}^{\text{UR}}\left(\phi_l^{\text{UR}}, r_l^{\text{UR}}\right)\boldsymbol{\alpha}_l, \\ \mathbf{a}^{\text{UR}}\left(\phi_l^{\text{UR}}, r_l^{\text{UR}}\right) \in \mathcal{A}\}, \quad (8)$$

where $\hat{\mathbf{h}} = \text{vec}\left(\hat{\mathbf{H}}\right) = \text{vec}\left(\mathbf{Y}\mathbf{X}^{\dagger}\right)$ is a vectorized version of the least square (LS) estimate of the channel [16], and $\boldsymbol{\alpha}_l$ is the complex amplitude. The infimum function implements minimizing the number of angles L such that we get the sparsest solution. The sparsest solution is the solution that contain only the exact angle ϕ^{UR} and distance r^{UR}. This problem can be thought of as if we constructed a dictionary matrix that contain all possible combinations of ϕ^{UR} and r^{UR}. Note that only the sparsest solution is valid and all the other solutions are redundant. Note that the problem formulated in (8) is considered an NP-hard problem that cannot be solved using traditional methods. Therefore, we relax the problem as follows: [17]

$$||\hat{\mathbf{h}}||_{\mathcal{A}} \triangleq \inf_{\boldsymbol{\alpha}}\Big\{ \sum_{l=1}^{L_{\text{tot}}} |\alpha_l| : \hat{\mathbf{h}} = \sum_{l=1}^{L_{\text{tot}}} \mathbf{a}^{\text{UR}}\left(\phi_l^{\text{UR}}, r_l^{\text{UR}}\right)\alpha_l, \\ \mathbf{a}^{\text{UR}}\left(\phi_l^{\text{UR}}, r_l^{\text{UR}}\right) \in \mathcal{A}\Big\}. \quad (9)$$

The new $||\hat{\mathbf{h}}||_{\mathcal{A}}$ given in (9) is called the atomic norm. The atomic norm can be used to solve the localization problem with the following objective function

$$\begin{aligned} \underset{\boldsymbol{\alpha},\mathbf{z}}{\text{minimize}} \quad & ||\hat{\mathbf{h}}||_{\mathcal{A}} \\ \text{subject to} \quad & \hat{\mathbf{h}} = \mathbf{U}\boldsymbol{\alpha} + \mathbf{z}, \\ & ||\mathbf{z}||_2 \leq \epsilon, \end{aligned} \quad (10)$$

where ϵ is noise threshold, and $\mathbf{U}$ is a matrix that contains all the possible combinations of ϕ^{UR} and r^{UR} which yield a semi-infinite programming problem. Solving the problem in (10) will result in a high-resolution estimation of the location.

B. the dual problem

Minimizing the primal problem in (10) is equivalent to maximizing the dual problem as strong duality hold. The first step to formulate the dual problem is to set up the Lagrangian as a weighted sum of the constraints with the objective function as

$$L(\boldsymbol{\alpha}, \mathbf{z}, \boldsymbol{\beta}, \boldsymbol{\gamma}) = ||\hat{\mathbf{h}}||_{\mathcal{A}} + \text{Re}\left[\boldsymbol{\beta}^H\left(\hat{\mathbf{h}} - \mathbf{U}\boldsymbol{\alpha} - \mathbf{z}\right)\right] \\ + \boldsymbol{\gamma}\left(\mathbf{z}^H\mathbf{z} - \epsilon^2\right), \quad (11)$$

where $\boldsymbol{\beta}$ and $\boldsymbol{\gamma}$ are Lagrange multipliers. The dual function $d(\boldsymbol{\beta}, \boldsymbol{\gamma})$ is the infimum of the Lagrangian and that is

$$d(\boldsymbol{\beta}, \boldsymbol{\gamma}) = \inf_{\boldsymbol{\alpha},\mathbf{z}} L(\hat{\mathbf{h}}, \boldsymbol{\beta}, \boldsymbol{\gamma}) = \inf_{\boldsymbol{\alpha},\mathbf{z}} \{\text{Re}\left[\boldsymbol{\beta}^H\hat{\mathbf{h}} - \boldsymbol{\beta}^H\mathbf{z}\right] \\ + \boldsymbol{\gamma}\left(\mathbf{z}^H\mathbf{z} - \epsilon^2\right) + ||y||_{\mathcal{A}} - \text{Re}\left[\boldsymbol{\beta}^H\mathbf{U}\boldsymbol{\alpha}\right]\}. \quad (12)$$

To solve (12), we first minimize over $\mathbf{z}$ as

$$\frac{\partial d(\boldsymbol{\beta}, \boldsymbol{\gamma})}{\partial \mathbf{z}} = -\boldsymbol{\beta} + 2\boldsymbol{\gamma}\mathbf{z} = 0, \quad (13)$$

that yields $\mathbf{z}^{\star} = \frac{\boldsymbol{\beta}}{2\boldsymbol{\gamma}}$. Similarly, the dual function maximized over the dual variable $\boldsymbol{\gamma}$ we get

$$\frac{\partial d(\boldsymbol{\beta}, \boldsymbol{\gamma})}{\partial \boldsymbol{\gamma}} = \frac{||\boldsymbol{\beta}^H||_2^2}{4\boldsymbol{\gamma}^2} - \boldsymbol{\epsilon}^2 = 0, \quad (14)$$

that yields $\boldsymbol{\gamma}^{\star} = \frac{||\boldsymbol{\beta}^H||_2}{2\boldsymbol{\epsilon}}$. Now the dual function reduces to

$$d(\boldsymbol{\beta}) = \text{Re}\left[\boldsymbol{\beta}^H\hat{\mathbf{h}}\right] - \epsilon||\boldsymbol{\beta}||_2 + \inf_{\boldsymbol{\alpha}}\left(||\hat{\mathbf{h}}||_{\mathcal{A}} - \text{Re}\left[\boldsymbol{\beta}^H\mathbf{U}\boldsymbol{\alpha}\right]\right). \quad (15)$$

In order to solve for the infimum in (15), consider that for every element α_i, we have $\text{Re}\left[(\boldsymbol{\beta}^H\mathbf{U})_i\alpha_i\right] = \text{Re}\left[(\mathbf{U}^H\boldsymbol{\beta})_i^H\alpha_i\right] = |(\mathbf{U}^H\boldsymbol{\beta})_i||\alpha_i|\cos(\psi)$. Now using the definition of the atomic norm in (9) we get

$$|\alpha_i| - \text{Re}\left[(\mathbf{U}^H\boldsymbol{\beta})_i^H\alpha_i\right] = |\alpha_i|\left[1 - |(\mathbf{U}^H\boldsymbol{\beta})_i|\cos(\psi)\right] \\ \geq |\alpha_i|\left[1 - |(\mathbf{U}^H\boldsymbol{\beta})_i|\right]. \quad (16)$$

For $|(\mathbf{U}^H\boldsymbol{\beta})_i| \leq 1$ the lower bound is non-negative and the infimum is zero, otherwise the infimum is $-\infty$. As a result, we can express (15) as

$$d(\boldsymbol{\beta}) = \text{Re}\left[\boldsymbol{\beta}^H\hat{\mathbf{h}}\right] - \epsilon||\boldsymbol{\beta}||_2, \quad \text{s.t.} \quad ||\mathbf{U}^H\boldsymbol{\beta}||_{\infty} \leq 1. \quad (17)$$

The dual problem of (10) can be reformulated as

$$\begin{aligned} \underset{\boldsymbol{\beta}}{\text{maximize}} \quad & \text{Re}\left[\boldsymbol{\beta}^H\hat{\mathbf{h}}\right] - \epsilon||\boldsymbol{\beta}||_2 \\ \text{subject to} \quad & ||\mathbf{U}^H\boldsymbol{\beta}||_{\infty} \leq 1. \end{aligned} \quad (18)$$

The constraints in (18) are again semi-infinite programming. Referring to [18], we define a trigonometric polynomial as

$$\mathbf{V}(\boldsymbol{\tau}) = \sum_{l=0}^{L-1} \beta_l e^{-j\tau_l} = \mathbf{a}(\boldsymbol{\tau})^H\boldsymbol{\beta}. \quad (19)$$

According to Theorem 4.26 in [18], if the following inequality

$$|\mathbf{V}(\boldsymbol{\tau})| < |\mathbf{R}(\boldsymbol{\tau})|, \quad (20)$$

is satisfied, then the following is true

$$\begin{bmatrix} \mathbf{Q} & \boldsymbol{\beta} \\ \boldsymbol{\beta}^T & \mathbf{1} \end{bmatrix} \succeq 0, \quad (21)$$

where $\mathbf{Q} = \boldsymbol{\beta}\boldsymbol{\beta}^H$. This can be proved using Schur's complement. According to Corollary 4.27 in [18], if we took a spacial case of $|\mathbf{R}(\boldsymbol{\tau})| = k$ then the following approximation is true

$$\begin{bmatrix} \mathbf{Q}_k & \boldsymbol{\beta} \\ \boldsymbol{\beta}^T & \mathbf{1} \end{bmatrix} \succeq 0, \quad (22)$$

where $\mathbf{Q}_k$ is a diagonal matrix of of all the diagonal elements equal to k^2. Now we can relax the constrains in (18) as

$$||\mathbf{U}^H\boldsymbol{\beta}||_\infty = \underset{k}{\text{minimize}}\ \ k \quad \text{s.t.}|\mathbf{U}^H\boldsymbol{\beta}| \leq k. \tag{23}$$

In our case $k = 1$. As a result, (18) can be re-written as a SDP

$$\begin{aligned} &\underset{\boldsymbol{\beta},\mathbf{Q}_k}{\text{maximize}} \quad \text{Re}\left[\boldsymbol{\beta}^H\hat{\mathbf{h}}\right] - \epsilon||\boldsymbol{\beta}||_2 \\ &\text{subject to} \quad \begin{bmatrix}\mathbf{Q}_k & \boldsymbol{\beta}\\ \boldsymbol{\beta}^H & \mathbf{1}\end{bmatrix} \succeq 0. \end{aligned} \tag{24}$$

Similar to (22), $\mathbf{Q}_k$ is a diagonal matrix such that $\text{tr}(\mathbf{Q}_k) = 1$.

C. User Localization

After solving the dual problem in (24), the localization parameters are to be estimated. We can use the following null spectrum to search for ϕ^{UR} and r^{UR} as

$$P(\phi^{\text{UR}}, r^{\text{UR}}) = \frac{1}{|\mathbf{a}(\phi^{\text{UR}} \otimes r^{\text{UR}})\boldsymbol{\beta}\boldsymbol{\beta}^H\mathbf{a}(\phi^{\text{UR}} \otimes r^{\text{UR}})^H|}. \tag{25}$$

In order to estimate ϕ^{UR} and r^{UR}, the objective function in (25) requires 2D grid search.

1) Iterative Method: : To reduce the computational complexity, we propose utilizing an iterative solution in which we relax (25) into a 1D grid search for ϕ_1^{UR} given a random r_0^{UR} followed by another 1D grid search for the r_1^{UR} given ϕ_1^{UR}. We repeat the same process for k of iterations to search for the optimal $\hat{\phi}^{\text{UR}} = \phi_k^{\text{UR}}$ given r_{k-1}^{UR} followed by a search for the optimal $\hat{r}^{\text{UR}} = r_k^{\text{UR}}$ given ϕ_k^{UR}.

2) Particle Swarm Optimization Algorithm: : We propose using particle swarm optimization (PSO) to solve (25). For the PSO, we create a set of particles such that every particles represents a certain angle and distance and we evaluate (25) at every particle location. We update the location of every individual particle based on its own location, its own optimal evaluation of (25), and the global optimal of (25) among all the particles. More specifically, let $\mathbf{x}_i$ represents the current location of a certain particle i, let $\mathbf{p}_i$ represents the best location of that certain particle i, and let $\mathbf{g}$ represents the best location among all the particles. Now we can update the particle i location using

$$\mathbf{x}_i(t+1) = \mathbf{x}_i(t) + \mathbf{v}_i(t+1), \tag{26}$$

where $\mathbf{v}_i(t+1)$ is the updated velocity vector of particle i that can be described using

$$\begin{aligned} \mathbf{v}_i(t+1) =& w\mathbf{v}_i(t) + r_1c_1\left(\mathbf{p}_i(t) - \mathbf{x}_i(t)\right) \\ &+ r_2c_2\left(\mathbf{g}(t) - \mathbf{x}_i(t)\right), \end{aligned} \tag{27}$$

where c_1 and c_2 are acceleration coefficients, r_1 and r_2 are random numbers distributed uniformly between 0 and 1, and w is inertia coefficient. Algorithms 1 summarize the PSO algorithm.

By taking the Hermitian transpose of the received signal in (1), i.e., $\mathbf{Y}^H$, The other angle and distance θ^{BR} and d^{BR} can be estimated by applying the same methodology.

The UE location can be estimated from the pre-estimated location parameters ($\hat{\phi}^{\text{UR}}$ and $\hat{r}^{\text{UR}}$). Given a known RIS location, the location of the UE $\mathbf{p}^{\text{U}} = [x^{\text{U}}, y^{\text{U}}]$, can be estimated as

$$\begin{aligned} \hat{x}^{\text{U}} &= \hat{x}^{\text{R}} + \tilde{d}^{\text{UR}}\cos\left(\tilde{\theta}^{\text{UR}}\right), \\ \hat{y}^{\text{U}} &= \hat{y}^{\text{R}} + \tilde{d}^{\text{UR}}\sin\left(\tilde{\theta}^{\text{UR}}\right). \end{aligned} \tag{28}$$

IV. RIS CONTROL

For this section, we utilize an iterative phase design in which we first estimate the localization parameters as described in the previous sections using a random phase design, then we use the estimated parameters to control the RIS phase matrix. In that regard, we aim to minimize the localization error by maximizing the signal-to-noise ratio (SNR). We derive the optimal phase design as [13]:

$$\begin{aligned} \theta_r^\star =& \left(N^{\text{U}}N^{\text{B}}\right)^{-1}\sum_{b,u}\Big[b\ \hat{\omega}^{\text{BR}} + b^2\hat{\gamma}^{\text{BR}} \\ &+ r\ \hat{\alpha}^{\text{BR}} + r^2\hat{\beta}^{\text{BR}} + r\ \hat{\omega}^{\text{RM}} + r^2\hat{\gamma}^{\text{RM}} \\ &+ u\ \hat{\alpha}^{\text{RM}} + u^2\hat{\beta}^{\text{RM}}\Big],\ \forall r \in \left\{1, 2, \cdots, N^{\text{R}}\right\}, \end{aligned} \tag{29}$$

where $\alpha^{\text{BR}} \triangleq f(\phi^{\text{BR}})$ and $\beta^{\text{BR}} \triangleq g(\phi^{\text{BR}}, r^{\text{BR}})$. Now we re-estimate the localization parameters utilizing the new phase design, and we use the new estimated parameters to re-control the RIS. We repeat this process until convergence. Algorithm 2 summarizes the overall proposed algorithm.

Algorithm 1 Particle swarm optimization (PSO) algorithm

Input: The Lagrangian multiplier $\boldsymbol{\beta}$.
Initialize: All particles positions $\mathbf{x}_i(0)$, all particles velocities $v_i(0)$, acceleration coefficients c_1 and c_2, the random numbers r_1 and r_2.
for $t = 1$: maximum generation **do**
  for $i = 1$: population size **do**
    if $P(\mathbf{x}_i) < P(\mathbf{p}_i)$ **then** $\mathbf{p}_i(t) = \mathbf{x}_i(t)$ **end**
    Update the velocity vectors using (27)
    Update the position vectors using (26)
  end for
end for
Output $P^\star(\phi^{\text{BR}}, r^{\text{BR}}) = P(\mathbf{p}_i)$

Algorithm 2 RIS-aided near-field localization via the atomic norm minimization

Input: The received signal $\mathbf{Y}$, the PRS $\mathbf{X}$, the RIS location $\mathbf{p}^{\text{R}}$.
Initialize: $\boldsymbol{\Theta} \leftarrow$ random phase design.
for $j = 1$ to J **do**
  Estimate $\hat{\mathbf{h}}$ using $\hat{\mathbf{h}} = \text{vec}\left(\mathbf{Y}\mathbf{X}^\dagger\right)$.
  Estimate $\boldsymbol{\beta}$ using (24).
  Estimate ϕ^{UR} and r^{UR} using (25).
  Use (29) to compute for $\boldsymbol{\Theta}$.
end for
Compute the UE location $\hat{\mathbf{p}}^{\text{U}}$ using (28).
Output $\hat{\mathbf{p}}^{\text{U}}$

V. NUMERICAL RESULTS

We present selected numerical results in this section. We model the noise as a thermal noise such that $\sigma_z^2 = B_t\, T_{\rm k}\, K$ where B_t represents the bandwidth, K is Boltzmann constant, and $T_{\rm k} = 290$ is the room temperature measured in Kelvin. We consider the temporal multiple sparse Bayesian learning (T-MSBL) algorithm to solve the CS problems which [19], we use [20] to solve for (24) and we use MATLAB to implement the PSO. The simulation parameters are presented in Table. I. Table. II shows the hardware specifications for the workstation that is used for simulation.

TABLE I: The simulation parameters.

description	parameter	value
frequency	f_c	28 GHz
Number of UE antennas	$N^{\rm U}$	10
Number of RIS elements	$N^{\rm R}$	100
path loss exponent	μ	2
Number of PRSs streams	$M^{\rm o}$	20
BS location	$\mathbf{p}^{\rm B}$	[0 0]
RIS location	$\mathbf{p}^{\rm R}$	[2.5 2.5]
UE location	$\mathbf{p}^{\rm U}$	[5 0]
Bandwidth	B_t	5 MHz
Power	P	0.5 Watt
Noise Thresould	ϵ	0.001

In Fig. 2, we compute the localization error for different SNRs at the BS. We vary the SNR value by changing σ_z^2. It can be seen from the figure that a lower localization error can be achieved by increasing both the SNR and the number of BS antennas. The results shows that the sub-cm level of localization error can be achieved using higher values of SNR and $N^{\rm B}$.

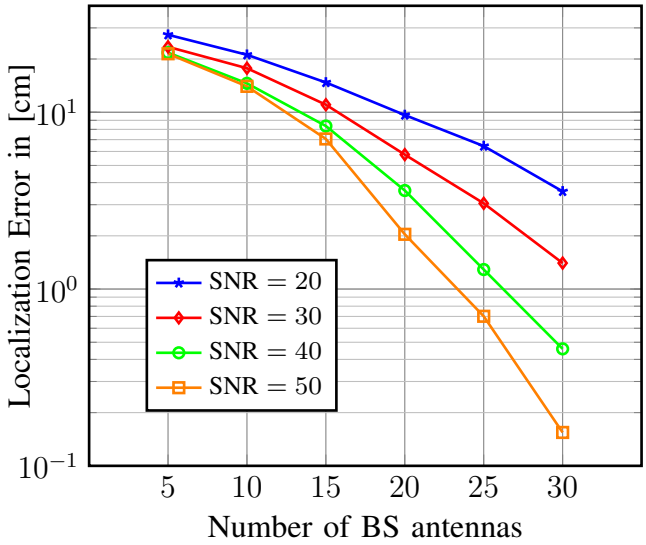

Fig. 2: Localization error aginst the numbers of BS antennas.

In Fig. 3, we compare the localization performance of the proposed atomic norm minimization with CS as a benchmark. We fix $N^{\rm B} = 35$ and we vary the number of RIS elements $N^{\rm R}$ and the number of the PRS streams $M^{\rm o}$. The results show the superior performance of the proposed atomic norm minimization in comparison to the CS. For instance, with $M^o = 20$ and $N^{\rm R} = 100$, the localization error can be reduced by 99.8% by achieving 0.1 cm localization error instead of 50 cm localization error when using our proposed algorithm compared to the CS methods. This can be justified as the CS utilizes a finite number of atoms on a discrete grid leading to a quantization error, while the proposed atomic norm uses a continuous set of atoms rather than a discrete one. The figure also shows that we can achieve better performance using a RIS with a large number of elements, as with larger $N^{\rm R}$ the RIS can make a narrow beam toward the UE location.

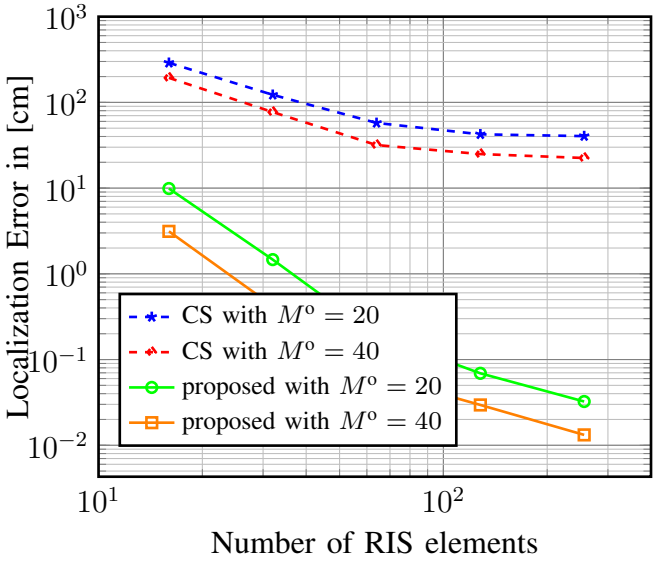

Fig. 3: Localization error comparison between the CS and the proposed scheme.

In Fig. 4, we compare the localization error for different optimization algorithms for solving (25), and we compare the exhaustive search (ES), particle swarm optimization (PSO), and the iterative solution described in section III-C. The figure shows a similar performance between the ES and the PSO while a slightly higher error for the iterative solution. To judge the performance of the three optimization algorithms, we compute the computational efforts for the three cases. Table. III represents the required time to solve for the UE location. The table shows that the iterative method can significantly reduce the required simulation time, however, it can produce a larger localization error. On the other hand, the PSO can produce the same localization accuracy as the ES but with lower computational effort.

TABLE II: Workstation specifications.

Aspect	Specification
CPU	Intel(R) Core(TM) i5-10500 CPU @ 3.10GHz 3.10 GHz
GPU	Intel(R) UHD Graphics 360
Memory	16.0 GB DDR4-SDRAM
OS	Windows 10 Education 64-bit

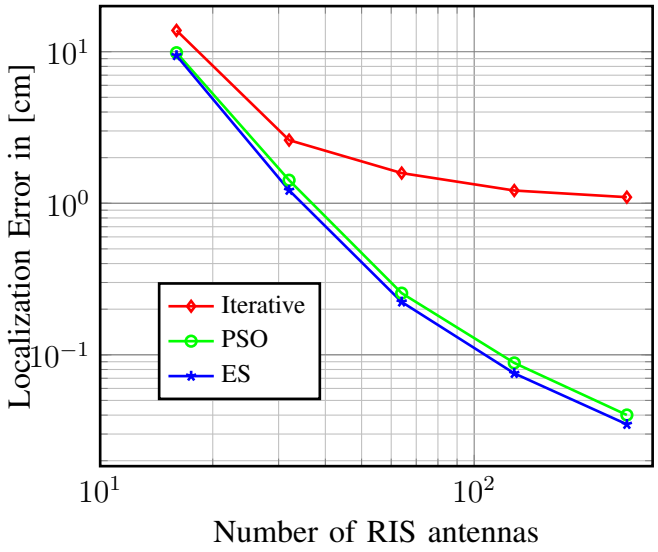

Fig. 4: Extracting the location parameters using different approaches.

TABLE III: Computational efforts.

Number of RIS elements N^{R}	Number of BS antennas N^{B}	Algorithm		
		PSO	ES	Iterative
		Time in [s]		
64	15	3.3115	3.9251	2.5414
	35	19.4865	26.4548	9.47864
128	15	4.4866	4.4698	3.4564
	35	21.4869	27.4856	10.4564

VI. CONCLUSIONS

In this paper, we propose a super-resolution RIS-aided localization scheme for single-snapshot localization in near-field environments. The localization relies on the atomic norm minimization and the numerical results show that a sub-cm error in localization can be achieved for some of the system configurations. These results can be used to extend this work in the future to address the localization problem for the near-field multi-path environments.

VII. ACKNOWLEDGMENT

This work was funded in part by Intelligent Systems Center (ISC) at Missouri University of Science and Technology (Missouri S&T).

REFERENCES

[1] C. De Lima, D. Belot, R. Berkvens, A. Bourdoux, D. Dardari, M. Guillaud, M. Isomursu, E.-S. Lohan, Y. Miao, A. N. Barreto, M. R. K. Aziz, J. Saloranta, T. Sanguanpuak, H. Sarieddeen, G. Seco-Granados, J. Suutala, T. Svensson, M. Valkama, B. Van Liempd, and H. Wymeersch, "Convergent communication, sensing and localization in 6G systems: An overview of technologies, opportunities and challenges," *IEEE Access*, vol. 9, pp. 26 902–26 925, Jan. 2021.

[2] A. Elzanaty, A. Guerra, F. Guidi, D. Dardari, and M.-S. Alouini, "Towards 6G holographic localization: Enabling technologies and perspectives," *arXiv preprint arXiv:2103.12415*, Feb. 2022.

[3] Y. Niu, Y. Li, D. Jin, L. Su, and A. V. Vasilakos, "A survey of millimeter wave communications (mmWave) for 5G: opportunities and challenges," *Wireless Networks*, vol. 21, no. 8, pp. 2657–2676, Apr. 2015.

[4] A. Araghi, M. Khalily, M. Safaei, A. Bagheri, V. Singh, F. Wang, and R. Tafazolli, "Reconfigurable intelligent surface (RIS) in the sub-6 GHz band: Design, implementation, and real-world demonstration," *IEEE Access*, vol. 10, pp. 2646–2655, Jan. 2022.

[5] H. Ibraiwish, A. Elzanaty, Y. H. Al-Badarneh, and M.-S. Alouini, "EMF-aware cellular networks in RIS-assisted environments," *IEEE Communications Letters*, vol. 26, no. 1, pp. 123–127, Oct. 2021.

[6] M. Di Renzo, A. Zappone, M. Debbah, M.-S. Alouini, C. Yuen, J. De Rosny, and S. Tretyakov, "Smart radio environments empowered by reconfigurable intelligent surfaces: How it works, state of research, and the road ahead," *IEEE Journal on Selected Areas in Communications*, vol. 38, no. 11, pp. 2450–2525, July 2020.

[7] A. Almasoud, M. Y. Selim, A. Alsharoa, and A. E. Kamal, "Improvement of bi-directional communications using solar powered reconfigurable intelligent surfaces," in *Proc. of the 30th International Conference on Computer Communications and Networks (ICCCN'21)*, Athens, Greece, July 2021, pp. 1–8.

[8] H. Zhang, N. Shlezinger, F. Guidi, D. Dardari, M. F. Imani, and Y. C. Eldar, "Near-field wireless power transfer for 6G internet of everything mobile networks: Opportunities and challenges," *IEEE Communications Magazine*, vol. 60, no. 3, pp. 12–18, Mar. 2022.

[9] E. Björnson, Ö. T. Demir, and L. Sanguinetti, "A primer on near-field beamforming for arrays and reconfigurable intelligent surfaces," *arXiv preprint arXiv:2110.06661*, Dec. 2021.

[10] A. Elzanaty, A. Guerra, F. Guidi, and M.-S. Alouini, "Reconfigurable intelligent surfaces for localization: Position and orientation error bounds," *IEEE Transactions on Signal Processing*, vol. 69, pp. 5386–5402, Aug. 2021.

[11] M. Rahal, B. Denis, K. Keykhosravi, B. Uguen, and H. Wymeersch, "RIS-enabled localization continuity under near-field conditions," in *Proc. of the 22nd IEEE International Workshop on Signal Processing Advances in Wireless Communications (SPAWC'21)*, Lucca, Italy, Nov. 2021, pp. 436–440.

[12] D. Dardari, N. Decarli, A. Guerra, and F. Guidi, "LOS/NLOS near-field localization with a large reconfigurable intelligent surface," *IEEE Transactions on Wireless Communications*, vol. 21, no. 6, pp. 4282–4294, Nov. 2021.

[13] O. Rinchi, A. Elzanaty, and M.-S. Alouini, "Compressive near-field localization for multipath RIS-aided environments," *IEEE Communications Letters*, vol. 26, no. 6, pp. 1268–1272, Feb. 2022.

[14] J. He, H. Wymeersch, and M. Juntti, "Channel estimation for RIS-aided mmwave MIMO systems via atomic norm minimization," *IEEE Transactions on Wireless Communications*, vol. 20, no. 9, pp. 5786–5797, Apr. 2021.

[15] B. Friedlander, "Localization of signals in the near-field of an antenna array," *IEEE Transactions on Signal Processing*, vol. 67, no. 15, pp. 3885–3893, Aug. 2019.

[16] A. Alwakeel and A. Mehana, "Achievable rates in uplink massive MIMO systems with pilot hopping," *IEEE Transactions on Communications*, vol. 65, no. 10, pp. 4232–4246, June 2017.

[17] W.-G. Tang, H. Jiang, and S.-X. Pang, "Grid-free DOD and DOA estimation for MIMO radar via duality-based 2D atomic norm minimization," *IEEE Access*, vol. 7, pp. 60 827–60 836, May 2019.

[18] B. Dumitrescu, *Positive trigonometric polynomials and signal processing applications*. Springer, 2007, vol. 103.

[19] Z. Zhang and B. D. Rao, "Sparse signal recovery with temporally correlated source vectors using sparse bayesian learning," *IEEE Journal of Selected Topics in Signal Processing*, vol. 5, no. 5, pp. 912–926, June 2011.

[20] M. Grant and S. Boyd, "CVX: Matlab software for disciplined convex programming, version 2.1," 2014.